Marine Pollution Bulletin 221 (2025) 118410

Contents lists available at ScienceDirect

Marine Pollution Bulletin

journal homepage: www.elsevier.com/locate/marpolbul

A statistical representation of oil spill fate in the Salish Sea (Part 2)

Rachael D. Mueller [a,b,c], Susan E. Allen [a,*], Stephanie Chang [d], Haibo Niu [e], Douglas J. Latornell [a], Shihan Li [e], Ryah Bagshaw [d], Ashutosh Bhudia [a], Vicky Do [a], Krista Forysinski [d], Ben Moore-Maley [a], Cameron Power [d]

[a] Department of Earth, Ocean, and Atmospheric Sciences; University of British Columbia, 2207 Main Mall #2020, Vancouver, V6T 1Z4, British Columbia, Canada
[b] Genwest Systems, Inc., PO Box 397, Edmonds, 98020, WA, USA
[c] National Atmospheric and Oceanic Administration, 7600 Sand Point Way NE, Seattle, 98115, WA, USA
[d] School of Community and Regional Planning and Institute for Resources, Environment and Sustainability; University of British Columbia, 433 - 6333 Memorial Road, Vancouver, V6T 1Z2, British Columbia, Canada
[e] Department of Engineering; Dalhousie University, 5217 Morris St, Halifax, B3j 1B6, Nova Scotia, Canada

ARTICLE INFO

Keywords:
Oil spill modeling
Monte Carlo
Salish Sea
Shipping risks
Indigenous reconciliation

ABSTRACT

We use a novel approach that combines Automatic Identification System (AIS) ship traffic data, state regulated oil transfer data, and a suite of numerical models to statistically represent the risk of spilled Alaska North Slope Crude, Bunker-C, and Marine Diesel under a variety of environmental conditions in an estuarine environment off the northeastern Pacific Ocean. We show the statistics of fate and transport outcomes based on 10,000 MOHID oil spill model simulations with currents, winds, and waves between January 1, 2015 and December 31, 2018. Each of the 10,000 oil spill scenarios was run individually and includes weathering from biodegradation, dissolution, dispersion, emulsification, evaporation, and spreading. Our pioneering approach captures statistical variability in seasonality, vessel traffic, spill locations, and oil types. We show that heterogeneity of 3D circulation in an estuarine environment, combined with marine traffic "footprints", creates regionally-variable signatures of the timing, likelihood and type of potential oiling.

1. Introduction

The Salish Sea is a semi-enclosed body of water located off the northeastern Pacific Ocean between Vancouver Island and the mainlands of the United States and Canada, within the territories of many Indigenous Nations. It supports 8,300 deep draft vessel transits (Van Dorp and Merrick, 2017), 45 billion liters of oil transported as cargo each year (Washington State Department of Ecology, 2020), and distinct oceanographic regions with different driving forces of surface and vertical transport. Although the Salish Sea has not yet experienced impacts from a major oil spill, both endangered species as well as a ~5 billion dollars economy in ecosystem services (Mackey et al., 2022) are vulnerable to a major spill incident. This paper aims to address this vulnerability by providing information on the likelihood of fate and transport from a major spill event within this unique physical environment.

Peer-reviewed research of numerical simulations on oil spill fate in the Salish Sea is sparse and focuses on past spill events or spills in particular locations. One case study in Puget Sound showed that two oil spill models (BLOSSOM and GNOME) produce similar results when using the same forcing (Duran et al., 2018). The study highlights the importance of tidal currents, winds, and turbulent diffusion on oil spill fate and transport, which translates to meaning that validating a model at one location does not guarantee the same performance in a different location because the Salish Sea is a dynamically rich environment with distinct, regional hydrodynamics that are not captured equivalently well amongst models. A model's performance in one region does not guarantee the same performance in a different region. Indeed, uncertainty in the model products used for wind, wave, and current forcing is a main source of known uncertainty in oil spill fate predictions (Keramea et al., 2021). One of the ways to address this uncertainty is by representing oil spill fate as a likelihood of impact based on the aggregated statistics from many runs rather than simply evaluating one trajectory.

In previous studies, statistical representations of oil spill fate were used to demonstrate the likelihood of impacts at 4 locations at or near the locations of perceived risk for oil spills by tankers (typically Aframax size) servicing Canada's Westridge Marine Terminal (Niu et al., 2017; Zhong et al., 2018; EBA Engineering Consultants, 2013; location

* Corresponding author.
E-mail address: sallen@eoas.ubc.ca (S.E. Allen).

https://doi.org/10.1016/j.marpolbul.2025.118410
Received 18 December 2024; Received in revised form 2 June 2025; Accepted 2 July 2025
Available online 30 July 2025

Table 1
Crude-oil transfer terminals in 2018, shown in Fig. 1.

Fig. 1 label	Name of marine terminal	Transfer direction
1	Westridge Marine Terminal	export
2	BP Cherry Point Refinery	import and export
3	Phillips 66 Ferndale Refinery	import
4	Shell Puget Sound Refinery	import and export
5	Marathon Anacortes Refinery (formerly Tesoro)	import and export
6	Alon Asphalt Company & Refining	export
7	SeaPort Sound Terminal & Refining	export
8	U.S. Oil	import and export

shown in Fig. 1 and described in Table 1). The industry oil spill models used in these studies (OSCAR and SPILLCALC) incorporate surface currents from 3D hydrodynamic models but are not 3D simulations of oil spill fate and only use the surface currents in simulations to predict surface oiling. A strength of these applications is that they give information on the likelihood of impact; however, the applicability of this information for the purpose of preparation, planning, and response is limited by lack of statistical variability in seasonality, traffic, spill locations, and oil types. These other aspects of statistical variability are important because – as mentioned previously – the Salish Sea has regional differences in physical forcings (winds, tides, and/or buoyancy gradients) that have seasonal and inter-annual variations, in addition to the seasonal and inter-annual variability in shipping traffic.

A challenge in assessing the risk of spills in the Salish Sea from these previous studies is a lack of transparency of the underlying assumptions and equations used to generate these model products. Placing any statistical product in context requires an understanding of the underlying assumptions and parameters of the statistical study. False interpretations from statistical results are likely without this context. In this study, we try to mitigate false perceptions of our statistical results by carefully documenting all aspects of our statistical method for generating spill scenarios (see Part 1 of this manuscript, Mueller et al., 2025), providing references for the models and the model parameterizations used in this study, including uncertainty (bootstrap method) and providing open access to the model output for winds, waves, and ocean currents.

There are additional challenges in statistically representing oil spill fate in the Salish Sea that go beyond accurately capturing the physical environment and relate to how to best represent oil spills, including information on spill locations, times, oil types, and volumes. Spill locations and times relate to maritime traffic accidents, which are driven by many factors (Aalberg et al., 2022; Council of Canadian Academies, 2016; Li et al., 2014; Chauvin et al., 2013). The Washington State Department of Ecology was tasked with reducing oil spill risks to Southern Resident Killer Whales (a local, endangered species) by developing an oil spill risk model based on traffic-accident likelihood from Automatic Identification System (AIS) ship traffic data. They succeeded in evaluating the efficacy of tug escorts in reducing risk by focusing on loss of propulsion events (Washington State Department of Ecology, 2023). Other spill risks include collisions, allisions, and sinking. Analyses of historical data indicate that vessel type and age of vessel are related to a higher probability of navigation accident, with cargo vessels being more likely to be involved in navigation accidents than other vessel types (Li et al., 2014; Aalberg et al., 2022). The amount of miles sailed and higher speeds (for larger ships) are also correlated with increased risk of accident (Aalberg et al., 2022). A ship traffic based model of spill risks in the Salish Sea could capture these nuances of shipping risk but has yet to be developed. Absent this model, an alternative approach is to characterize oil spill risks by the amount of time that vessels spend on the water (Vessel Time Exposure or "VTE", as described by Van Dorp and Merrick, 2017). We use this VTE approach and estimate the risk of spill location and month from AIS ship-track derived traffic density records and have documented this approach in Part 1 of this two-part manuscript (Mueller et al., 2025).

Other studies have taken an alternative approach to estimating risks from vessel traffic by completely avoiding the complexity of traffic risk and instead evaluating fate from specified locations with fixed volume sizes (Niu et al., 2017; Page et al., 2019; Zhong et al., 2018; EBA Engineering Consultants, 2013). Five different locations within the Salish Sea have been evaluated in this way (Niu et al., 2017; Page et al., 2019; Zhong et al., 2018; EBA Engineering Consultants, 2013). We chose a different approach because pre-selecting spill locations introduces a human bias in assuming where spill accidents will occur. In reality, the incidents that have either threatened or resulted in spills were not in these studied regions and include: a sunken push tug spilling 110 m^3 of diesel because the one person on the bridge fell asleep and the safety navigation alarms were not activated (presumably because a near-shore transit was desired), Transportation Safety Board of Canada (2016), Downing (2021); an uncoupling of a push tug from its oil tank barge carrying 4,000 m^3 of crude oil due to a mechanical failure of the push-pin coupling that was compromised by wave action (Ship-source oil pollution Fund, 2017); a gas tank left open after bunkering (Pawson, 2018), resulting in a continuous in-transit spill of 30 m^3; and an in-harbor spill of 2.7 m^3 that was attributed to a faulty valve and an improperly installed alarm system (Woodward, 2019). We chose a very simple traffic risk model based on 2018 Automated Identification System data to accommodate an "accidents happen" approach. Our goal was to remove human bias from our evaluation of potential impacts.

Although the information presented here may have been created with care to reduce human bias, the actual impacts from a major oil spill will have an inherent human bias toward impacting Indigenous communities more than other communities. Indigenous communities have engaged in subsistence living practices since time immemorial. Addressing potential harm to this subsistence living is an important aspect of reconciling past and present harm to these communities. We developed this research in tandem with learning how science and scientists can do better in helping to support efforts of reconciliation with Tribal/First Nations communities (see, e.g., Wong et al., 2020; Hare, 2021; Hauser et al., 2023; Kimmerer and Artelle, 2024). Aspects of this paper are intentionally crafted out of consideration for community needs and in response to community requests. Specifically, we provide a version of this paper in relatable units to U.S. Tribal communities (e.g. gallons, available upon request from the authors), we tailor scientific information to show impacts to locations of cultural importance, and we choose to publish in a way that will allow free access to this information. We also dedicate a discussion section (Section 4.4) to share the insights that we have learned in order to amplify the knowledge that we received and to help reduce the educational burden being placed on community researchers.

This paper describes the modeling framework (Section 2.1) and the aggregation of 10,000 spill simulations (Section 2.2) used to evaluate oil spill risk in the Salish Sea. It advances the approach in Fernandes et al. (2016) by including oil attribution from oil transfer data as well as model forcing from models that are used in Canada's oil spill response. The companion paper Mueller et al., 2025 describes the method for generating the 10,000 Monte Carlo spill scenarios, which we refer to as the Study Spill Set. Together, these papers explain a method for statistically generating 10,000 potential spill scenarios and predicting likelihood of impacts from the aggregated outcomes of these individual spill scenarios. Our results are generated with a numerical modeling suite for the purpose of planning and preparation to help prevent harmful impacts from a potential major oil spill in the Salish Sea (MIDOSS research team, 2024). Care has been taken to provide context for these results and to highlight knowledge gaps in our research in order to help facilitate accurate interpretations of the information presented here. The results of this paper (Section 3) are divided into explanations of oil spill fate, the presence of oil on the surface ocean, the presence of oil within the water column, coastal impacts by oil type, and coastal impacts by oil volume. Following results, we discuss in Section 4 our modeling limitations, the future of marine oil transport in the Salish Sea, asset planning, and reconciliation with Indigenous communities.

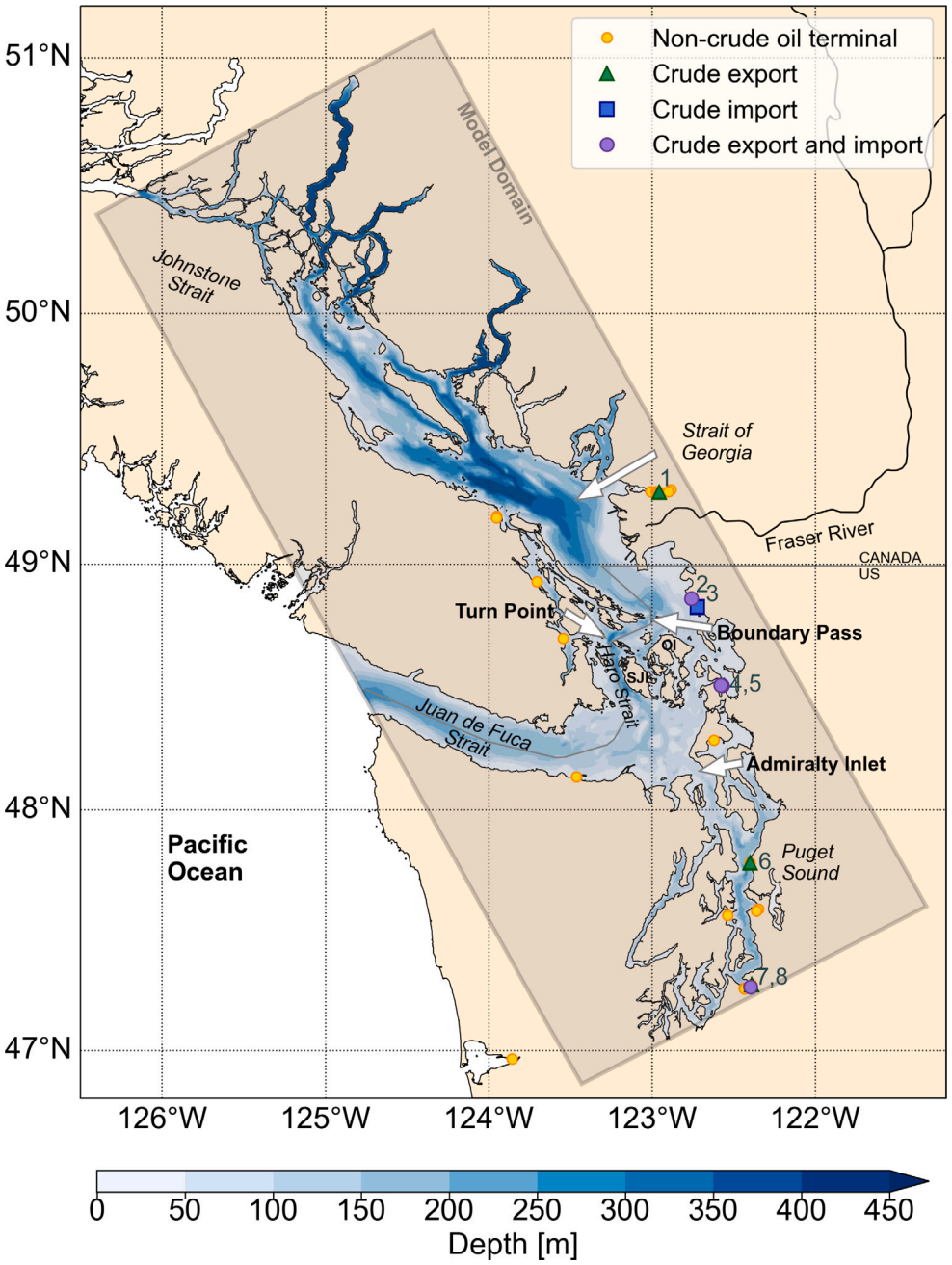

Fig. 1. Location of this study with the SalishSeaCast model domain and boundary for oil spills and oil spill fate shown in darker brown. The seafloor depth is shown in blue. The yellow dots mark the locations of non-crude oil transfer terminals while all other markers show crude oil transfer stations distinguished as: green triangles for crude export only, a blue square for crude import only, and purple circles for locations that import and export crude oil. The crude-oil terminals are listed in Table 1 according to the numbers shown in this graphic. In 2018, Washington crude-oil terminals reported oil transfers of Bakken, "crude oil", and/or Bitumen (Washington State Department of Ecology, 2020). Westridge Marine Terminal, BP Cherry Point Refinery (2) and Marathon Anacortes Refinery (5) receive light to heavy crude from the TransMountain pipeline. Westridge primarily exports heavy crude to California and Asia (Canada Energy Regulator, 2023).

2. Methodology

We statistically generated 10,000 spill scenarios (explained in Part 1, Mueller et al. (2025), and mapped in Fig. 2) to estimate the likelihood of oil spill impacts in the Salish Sea. The timing of these spill scenarios were weighted by vessel traffic with environmental conditions randomly chosen from model output between January 1, 2015 and December 31, 2018 in order to include as much inter-annual variability as we could. In this section, we provide details on the numerical modeling suite used to predict oil spill fate and our methods for aggregating the results.

2.1. Modeling framework

We modified the particle tracking oil spill model MOHID 2.1 (Neves, 2013; Marine and Environmental Technology Research Center, 2015; MIDOSS Research Group, 2018; Li, 2017) to estimate the fate of spilled oil based on dynamical predictions from a hydrodynamic model, an atmospheric model, and a wave model. We chose the NEMO model because it is open source and because of previous experience developing applications with it (Li, 2017). The hydrodynamic model is based on a NEMO 3.6 architecture and is referred to as SalishSeaCast (v201905, Soontiens et al., 2016; Soontiens and Allen, 2017;

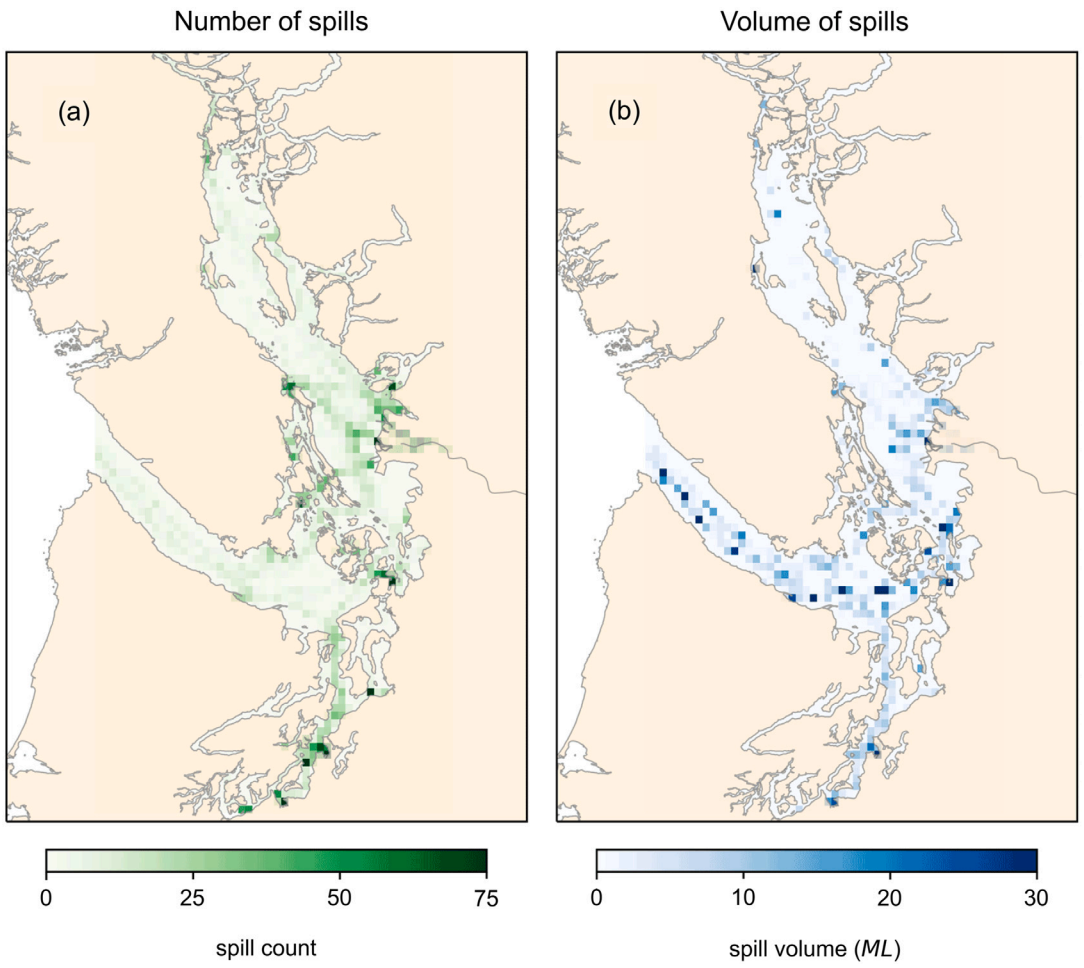

Fig. 2. Spill density maps of (a) spill count and (b) spill volume for the 10,000 spills evaluated in this paper.

Olson et al., 2020; Madec and the NEMO team, 2016). The wind model is 2.5-km-grid High-Resolution Deterministic Prediction System (HRDPS, Milbrandt et al., 2016; Environment and Climate Change Canada, 2019). The wave model is Wave Watch III® (Gemmrich and Pawlowicz, 2020), hereafter referred to as WW3. Our model domain is the extent of SalishSeaCast and is shown by the dark, shaded region in Fig. 1. The 2.5 km HRDPS and 1/12° WW3 model outputs are bilinearly interpolated onto the 500 m SalishSeaCast grid using the Spherical Coordinate Remapping and Interpolation Package (SCRIP) weighting matrix developed by Jones (2018). All forcing fields from SalishSeaCast, HRDPS, and WW3 are hourly averaged. SalishSeaCast provides the following fields: u-velocity, v-velocity, w-velocity, vertical diffusivity (K), sea surface height, time-dependent changes in model depth levels, sea surface temperature, and sea surface salinity. Wind forcing fields from HRDPS include both u- and v-wind components (10-meter equivalent). The WW3 model was used to provide information of wave period, wave height, whitecap coverage, significant wave height, mean wave length, u-stokes drift, and v-stokes drift. MOHID uses these model forcing fields as input for oil particle advection (MIDOSS Research Group, 2018). We ran each spill scenario for seven days using 2000, instantaneously released particles (Latornell et al., 2019). Spill volumes varied by spill according to the spills file produced by the Monte Carlo method described in Part 1 (Mueller et al., 2025; MIDOSS team, 2022). Horizontal transport was calculated every 3600 s (matches the hourly averaged hydrodynamics forcing) and vertical transport every 6 s (see Section 2.1.4 for more details on horizontal and vertical mixing).

Oil starts to change both chemically and physically upon being spilled and is affected by winds, waves, and ocean conditions. The chemical changes are referred to as weathering and are represented in this study as biodegradation, dissolution, dispersion, emulsification, evaporation. Weathering is applied uniformly across the spill every 60 s, based on averages of parameter values across the spill. The values used in these weathering algorithms are summarized in Table 2. The Coriolis Drift Angle is set to zero in the oil spill model because the effects of Coriolis are included in the physical forcing. We also do not include changes due to photodegradation or sedimentation. Crude oil, including Dilbit, is the type of oil most likely to be affected by sedimentation, and the regions most likely to be impacted by suspended particle interactions are river plumes during the spring freshet. In this study region, the three rivers that contain the highest amount of suspended particulate matter are the Fraser, Skagit, and Nooksack Rivers (Czuba et al., 2011). More details of the weathering algorithms used in this study are described in the following sections. Physical changes that can affect weathering, such as spreading and beaching, are also described in this section.

2.1.1. Beaching

In our model, weathering of oil stops once oil is beached and oil is not allowed to re-float after beaching. “On the coastline” is a more accurate description of “beached oil”, given that the Salish Sea coastline is not predominantly beaches; however, we rely on the term “beached” because it is the commonly used term to describe oiling along the coastline and is more succinct. We use these terms interchangeably in this paper. Oil has a 50% chance of beaching when it is within 250 m of the coastline.

Table 2
MOHID oil model parameter values with oil properties selected from Environment and Climate Change Canada (2022). Additional references are provided where appropriate.

General parameters	Diesel Fuel Canada	Alaska North Slope Crude	Bunker-C (IFO-380, Alaska)	Reference
Classification	Light Evaporator	Medium Floater	Heavy Floater	
Oil type	Refined	Crude	Crude	
API	39.4	29.9	11.4	
Pourpoint Temp. (°C)	−30	−54	−2	
Reference dynamic viscosity (cP)	2	16	8706	
Temp. of reference viscosity (°C)	15	15	15	
Weathering time step (s)	60	60	60	
Particle time step (DT, s)	3600	3600	3600	
Diffusion time step (δt, s)	6	6	6	
Weathering parameters	**Diesel Fuel Canada**	**Alaska North Slope Crude**	**Bunker-C (IFO-380, Alaska)**	
Beaching				
% likelihood	50	50	50	
limit (m)	250	250	250	
Evaporation				Fingas (2015)
Fingas equation	$(0.31 + 0.018\ \mathrm{SST})\sqrt{t}$	$(2.64 + 0.045\ \mathrm{SST})\ln(t)$	$(-0.13 + 0.013\ \mathrm{SST})\sqrt{t}$	
Dispersion				Johansen et al. (2015)
Oil–water interfacial tension (Dyne cm^{-1})	28	19.9	40	
Emulsification				Mackay (1980);
Emulsification parameter	–	1.60E−06	1.60E−06	Fingas (2011)
Max volume water content	0	62	35	
Evaporation threshold (%)	–	1.50E−06	1.50E−06	
Wax content	–	2.9	2	
Resin content	–	9	17	
Asphaltene content	–	5	11	
Saturate content	–	52	25	
Cemuls	–	1.5E−06	1.5E−06	
Biodegradation				Li (2017);
Analyte percentage (%)				Venosa and Holder (2007)
Group 1	7.4000E−01	1.3600E01	1.0000E−03	
Group 2	2.2600E00	2.6100E00	2.0000E−02	
Group 3	7.1100E01	8.2670E01	9.9820E01	
Group 4	2.5850E01	1.1300E00	9.0000E−02	
Group 5	3.0000E−02	1.0000E−02	0.0000E00	
Molecular weight (g $mole^{-1}$)				
Group 1	1.0411E02	9.2890E01	5.2250E−01	
Group 2	1.1975E02	1.0570E02	1.3075E02	
Group 3	2.1345E02	3.6875E02	4.5737E02	
Group 4	1.6301E02	1.7613E02	1.7228E02	
Group 5	1.3000E02	1.3000E02	1.3000E02	
Vapor pressure (atm)				
Group 1	1.2948E00	4.7889E00	3.0580E−02	
Group 2	6.1438E−03	2.4806E−02	2.7450E−03	
Group 3	2.0343E−04	1.0092E−04	6.5624E−06	
Group 4	4.2091E−06	2.8717E−05	3.0104E−05	
Group 5	6.9330E−04	6.9330E−04	6.9330E−04	
Solubility (ppm)				
Group 1	1.3135E01	2.3072E01	1.7271E−01	
Group 2	8.3274E01	3.4655E02	3.5000E01	
Group 3	8.1207E−06	5.3424E−06	4.2759E−07	
Group 4	5.7847E00	8.2596E00	8.7669E00	
Group 5	5.1000E04	5.1000E04	5.1000E04	
Biological coefficient (d^{-1})				
Group 1	1.0000E−01	1.0000E−01	6.0000E−04	
Group 2	1.0000E−01	1.0000E−01	1.0000E−01	
Group 3	1.6382E−02	1.0488E−02	5.3771E−03	
Group 4	1.9955E−02	2.9389E−02	2.9444E−02	
Group 5	5.0000E−03	5.0000E−03	5.0000E−03	
Wind correction parameters	**Diesel Fuel Canada**	**Alaska North Slope Crude**	**Bunker-C (IFO-380, Alaska)**	
Coriolis drift angle	0	0	0	
Wind transfer coefficient	2.70E−02	2.70E−02	2.70E−02	

2.1.2. Biodegradation

Oil biodegradation converts chemical constituents in oil into biological matter via microbial consumption. It occurs over longer timescales than the 7-day runs presented here, in a region where oil is most likely to reach the shoreline within three days (Pawlowicz et al., 2019); however, we include this weathering process nonetheless. We follow the works of Venosa and Holder (2007) and Lyman et al. (1982) in our representation of this process, as documented in Shihan Li's Master's thesis (Li, 2017). Oil molecules are divided into 5 groups by a combination of molecule type, biodegradation rate, and solubility. For each group, the input values of percentage, molecular weight, vapor pressure, solubility, and droplet biodegradation are calculated by adding up the values for each molecule within the grouping and weighting the molecule's value by the percentage of the oil represented by the molecule. The aggregated values that we used for the pseudo-component algorithm is shown in our biodegradation parameters supplementary document (Dataset S1). Biodegredation is set by the biodegradation rate determined for each of the five groups (Dataset S1). The algorithm is not a function of temperature or local, biological conditions, both of which can influence biodegradation rates.

2.1.3. Dissolution

Dissolution occurs when a fraction of soluble oil compounds dissolve into water and is important because the soluble compounds are the most toxic (Keramea et al., 2021). Different chemicals within oil have different solubilities. We partition the oil into five chemical groupings, each with different solubility rates. These are the same solubility rates and chemical groupings as those used in Section 2.1.2 and are outlined in Table 2. The dissolution rate (kg hr^{-1}) is estimated by:

$$\frac{dD_{diss}(n)}{dt} = k_c f_s A_s M(n) S(n), \quad (1)$$

where k_c=0.01 m h^{-1} is the dissolution mass transfer coefficient, f_s is the fraction of oil in the oil–water emulsion, A_s is the oil slick area (m^2, see Eq. (4)), $M(n)$ is the molecular weight of the analyte, and $S(n)$ (kg m^{-3}) is the oil solubility in water, calculated by:

$$S(n) = S_o(n)e^{-\alpha t}. \quad (2)$$

with $S_o(n)$ (kg m^{-3}) representing the solubility of the "fresh" oil for the five different chemical groupings (see Table 2), α a constant of decay (0.1 h^{-1}), and t is the time after spill (MARETEC, 2019). Total dissolved oil is the sum of dissolved analyte components.

2.1.4. Dispersion

We use the term dispersion as it is used in oil spill research, and not in the sense of diffusion for which we use the term mixing. Dispersion is the breaking up of the surface oil slick into droplets within the water column through turbulent mixing generated by waves and is a function of oil properties. The formation of these droplets is typically quantified using parameterizations developed from open-ocean, wind-generated waves (Keramea et al., 2021). In our version of MOHID 2.1, wave characteristics are estimated by averaged wind-wave states across the spill area. Once particles disperse below the surface layer, they are advected by vertical mixing processes. The vertical velocities of SalishSeaCast are not adequately resolved in the way that the horizontal velocities are (Allen et al., 2025), so we include SalishSeaCast vertical diffusivity (K) to capture vertical mixing from 3D circulation, inclusive of turbulence from tides. These vertical diffusivities inform a random walk following Visser (1997). The Visser method corrects a naive random walk approach to account for the particle drift that naturally occurs under the realistic conditions of turbulent dissipation varying with depth. This well-known vertical drift displaces particles from areas of lower diffusion toward areas of higher diffusion. The resulting particle displacement from ocean turbulence is characterized by a new particle depth (z_{n+1}) after partial time step δt that is described in Equation 6 of Visser (1997) as:

$$z_{n+1} = z_n + \frac{\partial K}{\partial z}\delta t + R\left[6K\left(z_n + \frac{\partial K}{\partial z}\delta t/2\right)\delta t\right]^{1/2}, \quad (3)$$

with K (m^2 s^{-1}) from SalishSeaCast vertical diffusivities and a time step (δt) of a random process (R) with uniform distribution and a standard deviation of 1/3 . We use DT = 3600 s. and t_{scale} = 600 such that $\delta t = DT/t_{scale}$ = 6 s, which satisfies the criteria of $\delta t \ll MIN(1/(\partial^2 K/\partial z^2))$. The random walk is repeated t_{scale} times for each model time step, DT. The vertical rise due to particle buoyancy is separate from the vertical motion due to vertical diffusivities and vertical velocities. All of these vertical displacement components are used in the calculation of particle depths. Although the movement of particles after being dispersed from the surface water into the water column is more related to particle advection, we mention our method of distributing particles within the water column here because of its relationship to surface dispersion.

2.1.5. Emulsification

Emulsification occurs when water is mixed into oil and can increase the volume of spills by up to three times (Fingas, 2011). The process of emulsification varies by oil type. Emulsions are more stable with oils that have higher levels of asphaltenes (Fingas, 2015), meaning that these oils will be more resistant to separating back to oil and water. Highly viscous oils may not uptake water and some medium crude oils may require some evaporation to concentrate asphaltenes enough to emulsify (Fingas, 2015). Refined oil does not absorb water and, hence, does not emulsify. In our model runs, we set emulsification to zero for the Diesel cases by setting the max volume water content to zero for this case (see Table 2). We use the Mackay (1980) emulsification algorithm for the Alaska North Slope Crude (ANS) and Bunker-C oil cases (see Equation 1 of Chapter 10 in Fingas (2011)). Table 2 summarizes values of asphaltene content, wax content, resin content, and saturate content.

2.1.6. Evaporation

Evaporation is the release of volatile compounds into the atmosphere. Different oil types have different amounts of volatile compounds and the rate of release of these compounds is a function of Sea Surface Temperature (SST) (Fingas, 2015). See Table 2 for a list of equations. The influence of wind on evaporation is not included in this study. For ANS and Bunker-C, 82% of the total evaporated mass over 7-days is lost in the first day, compared to only 45% for Diesel. After 3-days, these percentages raise to 94% and 77%, respectively. Diesel is the fuel type in our study that contains the most evaporate and has a non-negligible positive rate of evaporation after 7-days. In our model setup, evaporation (and all weathering) stops when beaching occurs.

2.1.7. Spreading

We use Fay's solutions (Fay, 1969; MARETEC, 2019) to estimate the initial area of a spill (A_s). This area is determined by the volume of spilled oil (V_o) and the differences in the densities of oil (ρ_{oil}) and water (ρ_w) as follows:

$$A_s = \frac{\pi}{4}\left(\frac{k_2^2}{k_1}\right)^2\left(\frac{(g'V_o^5)^{1/6}}{\nu^{1/3}}\right) \quad (4)$$

where k_1 and k_2 are 1.14 and 1.45, respectively (Flores et al., 1998, see also Table 2), g' is reduced gravity, $g' = (\rho_w - \rho_{oil})g/\rho_w$, and ν is the kinematic viscosity of water. SalishSeaCast temperature and salinity are used to calculate the density of water, ρ_w. The area of the spill changes in accordance with the evolving difference between $\rho_{oil}$and ρ_w. This area influences the amount of evaporation (weathering) and is not used to determine particle transport.

2.2. Aggregation of results

We use a bootstrap method to account for scenarios not captured by our Study Spill Set and to provide an error bound for our maps of likelihood. Consider Figures 10 and 11 in Part 1 (Mueller et al., 2025), which can be used to compare the spill count and spill volume of the three oil types in the Study Spill Set (Figure 10) with the variation of spill counts and spill volumes across all nine iterations (Figure 11). Added to this variability in spill count and volume is an inherent range of wind and current conditions that would affect the outcome of any given spill scenario. The bootstrap method is the best approach for capturing this range of plausible outcomes, short of running more than 10,000 spills. Following the method described in Najmi (2015), we use a Poisson distribution to create 49 different spill weightings. These outcomes, plus the equal weighting for all spills, gives N=50 maps of oil presence, volume, arrival time, and dispersion depths that represent different plausible outcomes than those of the Study Spill Set. These variations are used to evaluate the error inherent in only sampling 10000 spills and to represent the likelihood of the given outcomes (Allen, 2021).

Results are aggregated to approximate the most likely value. A mean value will skew the results because the distribution of oil concentrations is not uniform, meaning that there are many small spills and only a few large spills. In order to best approximate a most likely concentration, we create a nearly Gaussian distribution by log-transforming the oil

concentrations and then calculate the mean based on these more Gaussian, log-transformed values. This calculation is known as a geometric mean. We apply a geometric mean calculation across spills where oil is present in the given grid and then un-transform the values prior to graphing in order to represent the most likely oil concentration with values that are easier to comprehend.

Variability across possible outcomes of geometric mean is estimated using quartiles from the randomly generated 50 bootstrap instances and presented as the Interquartile Range, or difference between the 75th (third quartile) and 25th (first quartile) percentiles of these instances. We do not show results for geometric mean oil concentrations if the difference of the third to first quartile is larger than the mean. In addition, the depth of the dispersed oil is only shown if the difference of the third to first quartile is larger than 5 m and 25% of the mean of bootstrap estimates.

Thresholds are used to limit our analyses to only include times and locations with oil above volume and concentration levels that would cause socioeconomic impacts, like loss of food. For oil on the surface, we define oil as present if the volume within a grid box is greater than 3 liters. This threshold corresponds to a socioeconomic impact threshold of 0.01 g m^{-2} (Reich et al., 2016; Dillon Consulting, 2017) within a grid box area of 0.25 km^2. For the coastline, we set our threshold to be 5 liters with the assumption of a swash zone of 6 m, and a coastline length per grid cell of around 800 m, to establish the socioeconomic threshold of 1 g m^{-2} (e.g. Table 9 in Dillon Consulting, 2017) for the oil types used in this study. For presence/absence, we estimate the probability of oil presence, p, given a single spill, as the number of spills with presence in that grid cell divided by the total number of spills, N. Our confidence in this estimate is calculated as:

$$2\left(\frac{p(1-p)}{N}\right)^{1/2}$$

which, given that $p \ll 1$, is approximately $2(p/N)^{1/2}$.

We calculate the time of arrival as the geometric mean, across all oil spills that have oil presence in a given grid cell. We apply the same bootstrap method as described above. We do not show beaching time if the difference of the first to third quartile is larger than half a day, or if it is larger than 25% of the mean arrival time.

3. Results

We evaluate the impacts of Salish Sea oil spills based on the aggregated results of the Study Spill Set of 10,000 spill scenarios (shown in Fig. 2, explained in Mueller et al., 2025). We start by describing the location of oil at the final time step (see code Mueller et al., 2018a,b). We then explore the presence of different types of oils, separately and then combined, in different regions of the Salish Sea. Lastly, we focus on the oiling of the coastline and explore: the presence of different oils along the coastline, the average time to oiling, and the spill locations that do or do not affect coastline oiling within specific regions. The iteration of 10,000 spills evaluated here only had 1 Dilbit spill, so we omit Dilbit from this evaluation and focus here on the three categories of Bunker-C, Diesel, and ANS. These results represent 3447 Bunker-C spills, 6405 Diesel spills, and 66 ANS spills. Table 5 in Part 1 has more information on the oils represented by these oil type attributions.

3.1. Oil spill fate

The four locations of oil spill fate evaluated in this study are: the water column (a combination of dispersed, biodegraded, and dissolved oil), the water surface, on the coastline, and in the air. Here, we use "on the coastline" to describe "beached oil", given that the Salish Sea coastline is predominantly rocky. The mass of oil along the coast (M_{coast_oil}) is calculated as:

$$M_{coast\_oil} = V_{coast\_oil}\left(\rho_e \frac{f_{m\_oil}}{f_{v\_oil}}\right) \quad (5)$$

where V_{oil} is the volume of oil on the coastline, ρ_e is the density of the oil and water emulsion, f_{m_oil} is the oil mass fraction, and f_{v_oil} is the oil volume fraction. If a mass of oil lands on the coastline at any time step then it remains beached for all subsequent time steps.

The fate of oil across the 10,000 oil spills represented in this study and binned by oil type is shown in Fig. 3. The three bars for ANS, Bunker-C, and Diesel represent the median of the percent of mass in each of the four fate locations, across all spill scenarios. The lower bound of the error bars represents the 0.25 quantile and the upper bound of the error bars represents the 0.75 quantile. Very little mass remains in the water column or on the water surface by the end of our spill scenarios. Most oil mass ends up along the coastline and some is evaporated. Diesel evaporates the most, at around 30% of its mass, while Bunker-C evaporates less than 10% of its mass.

The fate of Diesel is the most variable in our simulations because our model setup allows for evaporation when on the surface of the ocean and stops evaporation upon beaching. The variation in Diesel fate across all runs likely reflects a variation in beaching time scales across all runs. In contrast, across all runs, Bunker-C is most likely to end up on the coastline with very little evaporation or dispersal.

3.2. Surface presence of oil

We evaluate the presence of oil on the surface by tracking the location of oil movement during the duration of the spill and counting oil as being present in a grid cell (at any time during the spill) if the oil volume is greater than 3 liters. Oil presence is shown by oil type because different oils pose different challenges for recovery. Fig. 4 shows the total number of spills where oil is present above 3 liters. Generally speaking, there are two significant "hot spots" for oil presence. For Bunker-C, the most widespread area of oil presence is in the eastern Juan de Fuca and Haro Straits. There is also an amplified likelihood of presence of spilled oil just north of Orcas Island (O.I. in Fig. 1) and extending toward Boundary Pass. Although Diesel shows a similar pattern with these two "hot spots" the surface presence of Diesel is more consistent across runs in the area north of Orcas Island. In contrast, the surface presence of ANS is greatest along the Canadian side of the eastern Juan de Fuca Strait. Surface oil presence in the Puget Sound is significantly less than in regions to the north because oil spills in the Puget Sound are on the surface for a much shorter timescale before beaching. As such, the number of spills that circulate across any given grid cell in the Puget Sound are less than, for example, the eastern Juan de Fuca Strait, where there is more distance to shore and a longer time scale between oil release and beaching. In addition, the general circulation across Admiralty Inlet follows estuarine exchange, with surface currents moving seaward and away from the Puget Sound.

3.3. Vertical distribution of oil in water

Fig. 5 shows the number of spills where oil is present on the surface and in the water column as well as the averaged depth, in meters, of dispersed oil. With all oils combined, the greatest presence of oil across all runs is along the Canadian side of Juan de Fuca and Haro Straits (Fig. 5a). This is also an area that has a larger presence of oil in the water column than many other areas in the Salish Sea (Fig. 5b). The presence of oil in the water column is also more likely through Haro Strait and north of Orcas Island, across Boundary Pass. Turn Point and Boundary Pass are regions of strong tide convergent fronts with elevated vertical diffusivities. This tide-dominated circulation is reflected in the deeper dispersion depths from Boundary Pass to Turn Point and then southward through Haro Strait (Fig. 5c). The depth of dispersed oil is also deeper through Admiralty Inlet, which is another location of strong vertical mixing due to tides.

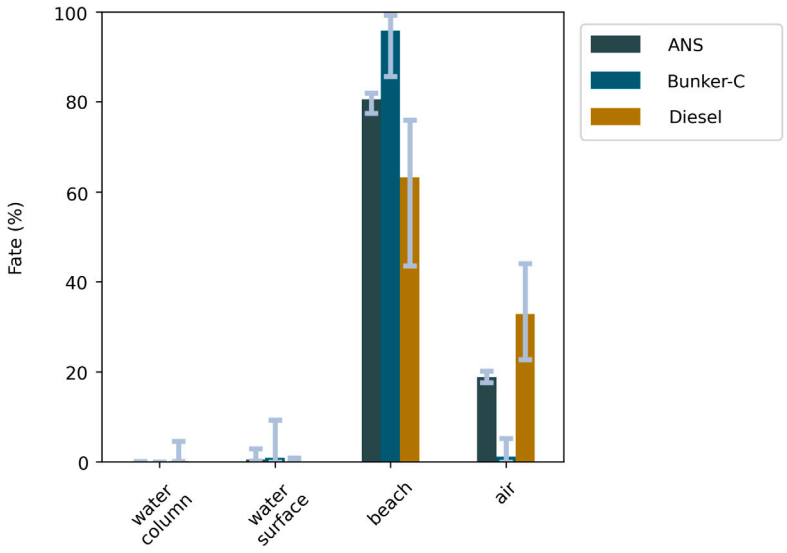

Fig. 3. Fate of all oil in spill scenarios according to the final mass balance at the end of each run scenario. The three bars for ANS, Bunker-C, and Diesel represent the median values across all spill scenarios of the percent of mass in each category. The lower bound of the error bars represents the 0.25 quantile and the upper bound represents the 0.75 quantile.

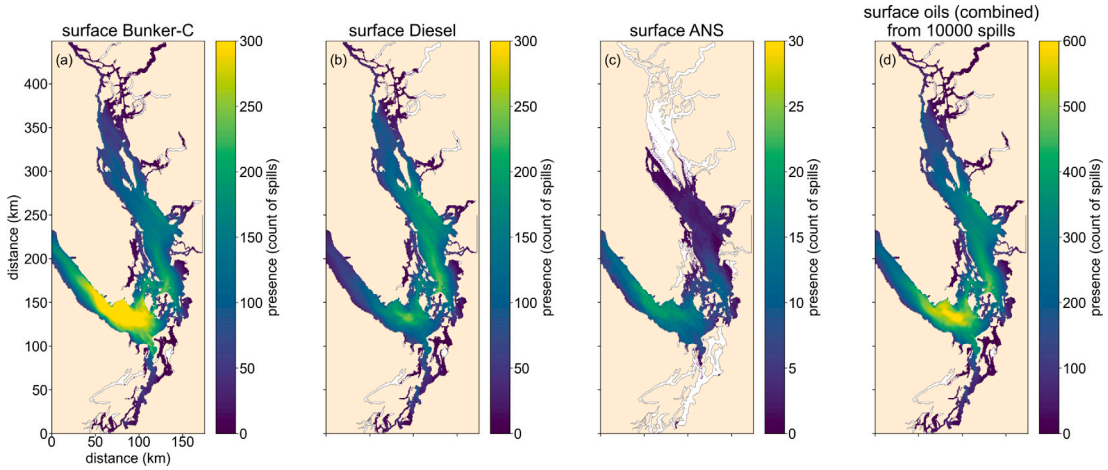

Fig. 4. Aggregated presence of water surface oiling greater than 3 liters within each grid cell at any time during the oil spill simulation, represented as a count of spills where oil is present for (a) Bunker-C spills, (b) Diesel spills, (c) Alaska North Slope Crude (ANS) spills, and (d) all 10,000 spills.

3.4. Coastal impact by oil type

Fig. 6 shows the likelihood of oiling by oil type based on the presence of oils on the coast, aggregated over all the runs. Oil presence is only counted in grid cells with 5 liters of oil, or greater than the socioeconomic impacts threshold of 1 g m^{-2} (Dillon Consulting, 2017). ANS is the least likely oil type to impact the coastline due to the lower probability of spills from this oil type (as reflected by the lower number of spills). ANS presence along coastlines is most likely through the Juan de Fuca Strait, Admiralty Inlet, San Juan Islands (OI, SJI, and nearby islands south of Turn Point in Fig. 1), and Anacortes, though it also shows up around the Ferndale shoreline and in parts of the Strait of Georgia (Fig. 6a). Bunker-C has a similarly strong presence through the Strait of Georgia and around San Juan Island, with higher likelihoods in the South Sound and parts of the Strait of Georgia (Fig. 6b). The presence of Diesel along the coastline is less likely through the Juan de Fuca Strait than other areas of Puget Sound, San Juan Islands, Gulf Islands (the islands north of Turn Point), and northern Strait of Georgia (Fig. 6c). Very few spots along the coast show zero likelihood of oiling, with all oils combined (Fig. 6d).

3.5. Coastal impact by volume of oil type

We estimate the representative oil volume to impact coastlines by using the geometric mean of beached oil volume across all runs, according to the oil type and runs affecting a particular location. Fig. 7a shows that ANS has the greatest volume to impact the coastline relative to Bunker-C and Diesel (Fig. 7b and 7c, respectively); however, we note that ANS is also the oil type least likely to impact the coast (Fig. 6a). In Part 1 of this study, Mueller et al. (2025), their Figure 10 shows the spatial distribution of spill count and spill volume by oil type for the Study Spill Set evaluated in this paper. Panel (f) of this Figure 10 reveals a series of larger spills (around 20 ML) through the Strait of Juan de Fuca. The location of these larger spill volumes reflects crude shipping in this region in 2018, which was before the completion of the Westridge Marine Terminal expansion and predominantly a result of ANS imports to Washington refineries north of the Puget Sound. The larger volumes are indicative of the ANS cargo being transported by vessels that have a larger capacity (see Figure 6(c) in Mueller et al., 2025). For the other oil types with spills that are more broadly distributed across this region (panels (d) and (e) of Figure 10 in Mueller et al., 2025), the coastlines with the largest median volumes (Fig. 7) also have a

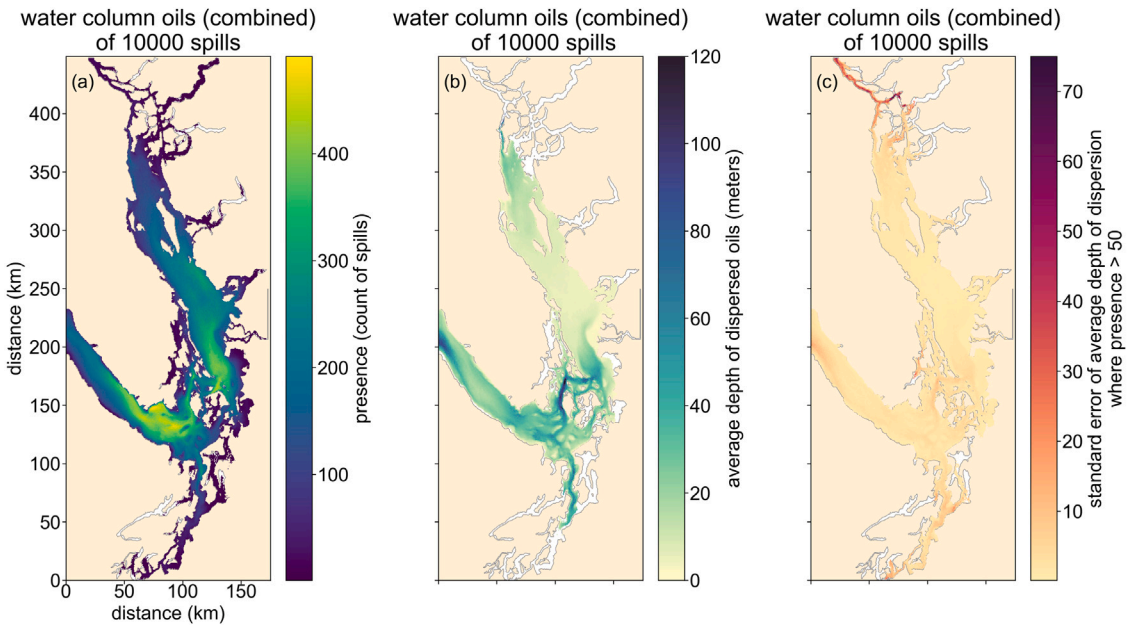

Fig. 5. Presence of oil in the water column across all 10,000 spills and represented as: (a) Number of spills within each grid cell where oil volume exceeded 3 liters at any time during the oil spill simulation, (b) average mean depth of dispersed oil where the difference of the first to third quartile of the bootstrap distribution is smaller than 5 m, or it is smaller than 25% of the mean depth, and (c) the difference between the third and first quartiles of the bootstrap distribution for mean depth.

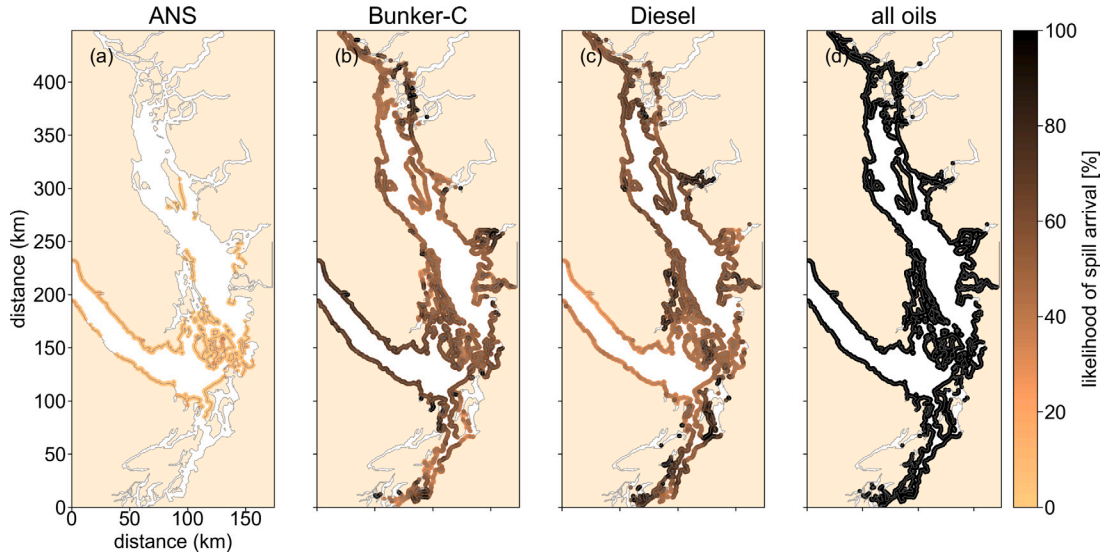

Fig. 6. Regional variations in oil spill fate as shown by the percent of spills to ground with greater than 5e-3 m^3 along 500 m of coastline for: (a) ANS, (b) Bunker-C, (c) Diesel, and (d) All oils.

shorter impact timescale (Fig. 8, discussed in the following section). This relationship between median volume along shorelines and timing of shoreline impact may be a consequence of our model setup, which stops evaporation once beaching occurs (see Section 2.1.6). Diesel has the highest fraction of volatile compounds and would, therefore, show the largest over-estimate of likelihood in shoreline volume impacts due to the termination of evaporation while on the shoreline.

3.6. Coastal impact by timing and distance

Maps of the average time to initial beaching of the different oil types along coastlines (Fig. 8) show that, in general, more narrow inlets and passages experience a smaller beaching time scale than areas where ship traffic is farther away from the coastline. There are some exceptions to this rule, however. The southern Strait of Georgia has a mean average beaching time of around 3 days versus 4 days in the more narrow and northerly part of the Strait. As a general rule of thumb, the closer a spill is to a shoreline the more quickly it will impact that shoreline; however, ocean and atmospheric conditions introduce outliers and heterogeneity to this rule. We show this heterogeneity by selecting four different regions and showing the spill locations that resulted in coastline oiling within these regions (Fig. 9a–d) as well as the spill locations that did not result in coastline oiling within the bounded region (Fig. 9e–h). Protecting shorelines in these and other regions will require a holistic approach that considers the influence of 3D circulation in affecting oil spill fate and transport. A possible exception to this need is south of Admiralty Inlet, in the Puget Sound, which is a longer and more narrow circulation corridor with strong tidal mixing across the northern entrance, which acts like a fluid barrier. Winds and timing of slack tide may overcome this barrier; but,

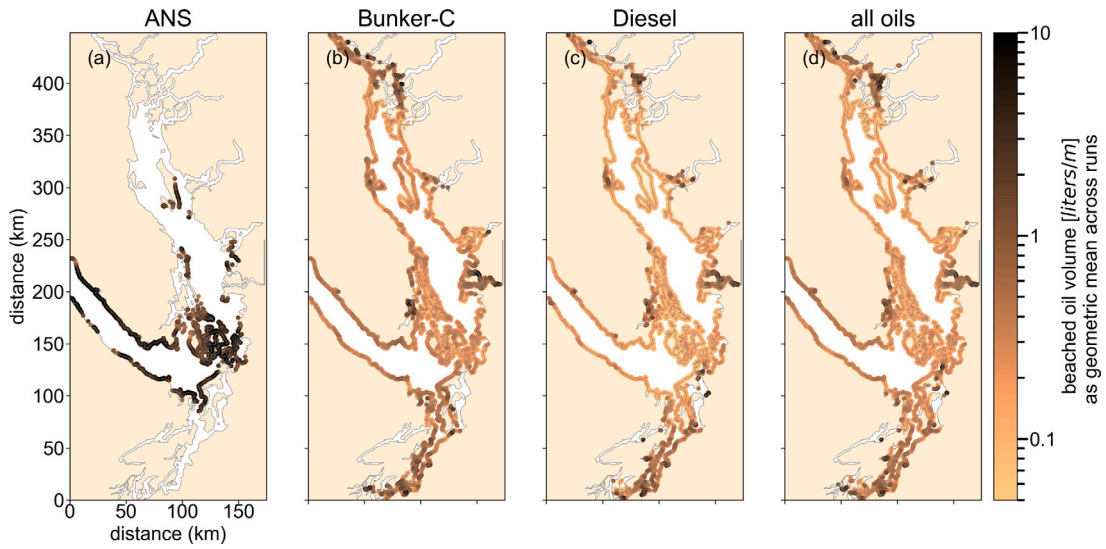

Fig. 7. Regional variations in oil spill fate as shown as the geometric mean volume of oil to beach along coastline for: (a) ANS, (b) Bunker-C, (c) Diesel, and (d) All oils.

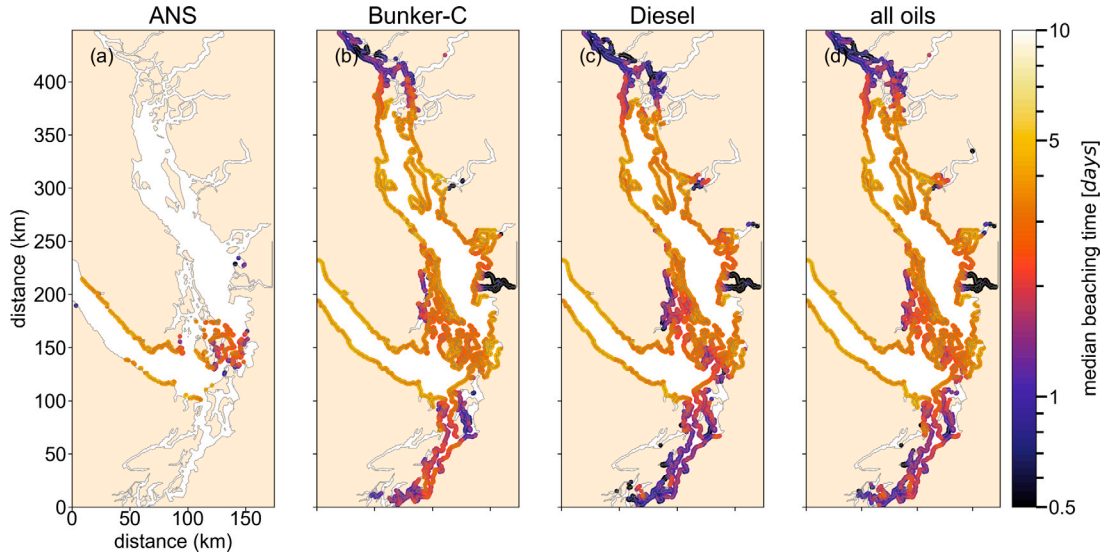

Fig. 8. Geometric mean (median) across all spills in the Study Spill Set of the length of time between the spill time and the initial contact with coastline.

in general, the timescale to beaching is shorter and the influence of circulation in advecting spills over a greater distance is less than in Haro Strait and the Strait of Georgia.

4. Discussion

Salish Sea ocean circulation is three-dimensional with regions that are distinct in how they are forced by tides, buoyancy, winds, and estuarine exchange flow. Until this study, the impacts of ocean circulation on oil spill fate in the Salish Sea had not been sufficiently investigated to allow for oceanographically-informed oil spill response plans in this region. A goal of this study was to address this need. We used AIS ship track data, oil transfer data, and a suite of numerical models to create a statistical estimate of oil spill fate in the Salish Sea.

In this section, we discuss aspects of our methods and results that we see as important to understand in order to achieve an accurate interpretation of our results. Section 4.1 explains how model parameterizations and setup may have biased our results, and we highlight necessary science and technological advancements needed to address knowledge gaps and/or deficiencies. Section 4.2 discusses the future of oil transport in the Salish Sea. In Section 4.3, we explain the likelihood of coastal oiling in the context of preparation and planning to help support preparedness activities. Lastly, in Section 4.4, we discuss our responsibilities as researchers to advance reconciliation with Indigenous communities.

4.1. Modeling limitations

Three modeling platforms were used to generate required inputs for MOHID oil spill fate predictions: (1) SalishSeaCast for temperature, salinity, surface currents, vertical velocities, and vertical diffusivities; (2) HRDPS for 10-m wind speeds; and (3) WW3 for significant wave height (H_s), wave period (T_s), white cap coverage (WCC), and Stokes drift (as described in Section 2.1). To our knowledge, no other study of oil spill fate in this region has included 3D transport, model diffusivities, or wave model inputs. Our modeling product may represent the most comprehensive physical forcing of any published oil spill study in this region, but model development is still needed. Here we discuss the limitations of our approach and the areas we see as most needing further development.

One area in need of advancement is the representation of 3D oil fate and transport. In this study, hourly-averaged 3D ocean circulation,

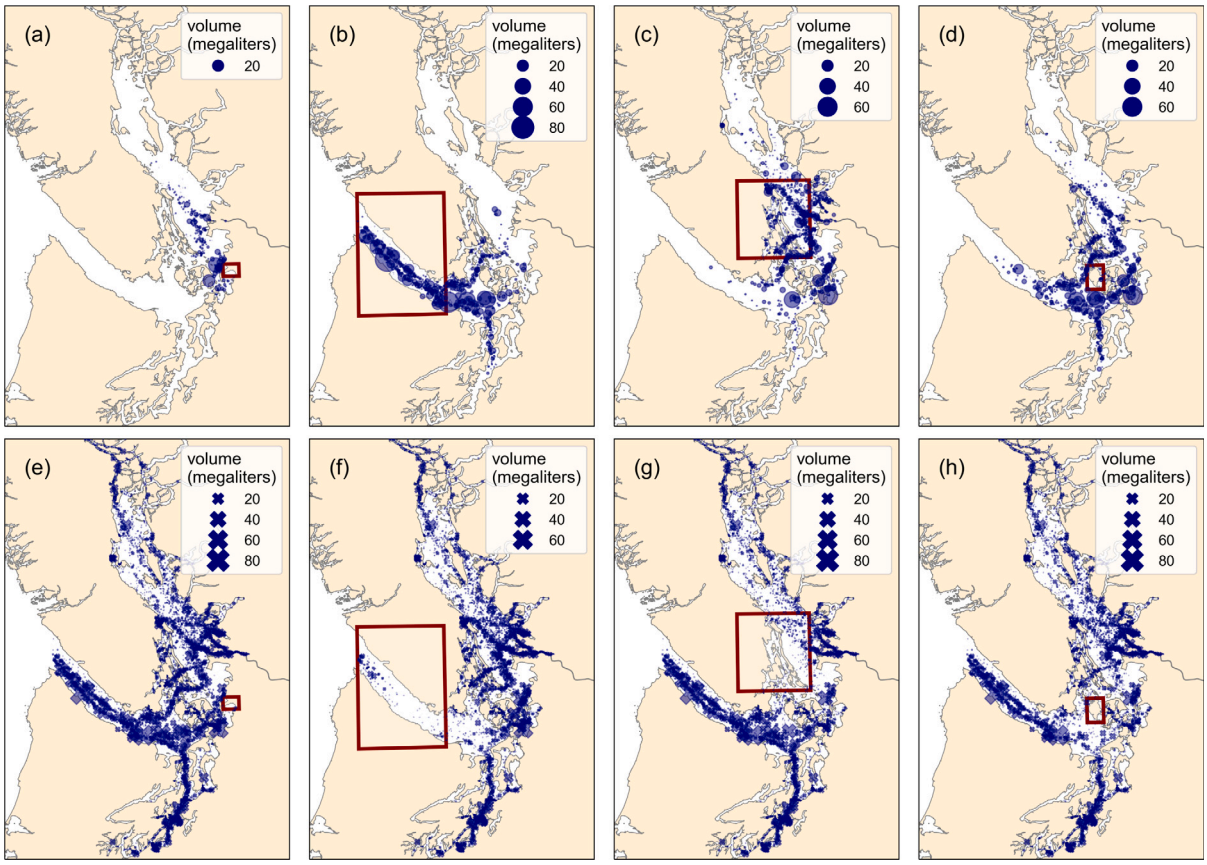

Fig. 9. (a–d) Spill locations and volumes affecting selected coastlines compared to (e–h) spill locations and volumes that do not impact selected coastlines. Red boxes enclose the selected coastlines. We encourage readers to explore the mapping website Native Land Digital (2023) to learn about the Indigenous communities within these regions.

wind, and wave forcing fields are used to inform oil spill fate and transport; but MOHID incorporates these fields differently for advection than it does for weathering. For advection, each particle is moved according to the 3D hydrodynamic, wind, and wave values at the individual particle's location. For weathering, on the other hand, only one value is used across all particles to characterize the physics used to advance weathering. Originally, this value was the position of the first particle, but we updated the code to use spatially averaged conditions across all particle locations instead of a value from only one of the particle locations. Every 60 s, weathering for all particles is advanced uniformly based on the spatially averaged fields. If a spill is spread across a large enough region that the wave height changes significantly, then the dispersion will be underestimated for some particles and overestimated for other particles as a result of this uniform weathering application. Effectively, this spatial averaging lowers the resolution of weathering and how weathering is affected by model inputs. A likely assumption when this model was developed was that wind speed, WCC, and other weathering inputs do not vary enough over the spatial scale of a spill (particularly in an open ocean environment) to introduce significant error. Even if this error is small relative to other uncertainties, we consider this aspect of the weathering model to be a limitation worth mentioning, particularly in this application where marine conditions vary over shorter space scales than they do in the open ocean environment. That said, uniform advancement of dispersion across all particles likely introduces a lesser error than the use of a dispersion algorithm that was developed for open ocean conditions and that only includes the influences of turbulent mixing due to tides once particles are dispersed below the surface and subjected to SalishSeaCast vertical diffusivities (Section 2.1.4). A dispersion algorithm for regions with strong currents in areas of tide convergent fronts has not yet been published, and we expect that our dispersion estimates underestimate naturally occurring dispersion in this region.

In addition to underestimating oil in the water, we also overestimate oil on the coastline. This overestimate of oil mass on the coastline is caused by our model setup in which oil stops weathering when it is flagged as beached and is not allowed to resuspend. In a real spill event, beached oil will continue to weather (e.g. evaporate) and may resuspend with changes in water height. Our prediction of the mass of oil onshore is biased high because we do not allow weathering processes to continue after reaching the shoreline. This bias is likely the most for Diesel, which has the greatest percentage of volatile compounds of all oils included in this study.

A regional consideration (primarily near the Fraser and Skagit Rivers) is the sedimentation that may occur as a result of interaction between suspended particulate matter and heavy crude oils, like Dilbit. Periods of high discharge (e.g. spring freshet) tend to correspond to a greater amounts of suspended particulate matter, which increases the likelihood of sedimentation. Funding for this study went toward developing a model for Dilbit oil mineral aggregation and sedimentation (Zhong et al., 2022), but this parameterization was not developed in time to be used in these model runs. As such, we exclude sedimentation in our predictions of oil spill fate.

Beyond model advancements, we also recommend a greater degree of transparency around models and their applications. It has become standard practice to present oil spill modeling results with little to no information on model setup, forcing, and equations because most of this work is proprietary and achieved through private consultation, outside of peer-reviewed, open-access research. A natural consequence of this lack of transparency can be an overconfidence in model results and/or mistrust of them. Both outcomes are undesirable because models can be useful tools for providing insights that can help support planning and preparation to help minimize impacts, especially in environments where we cannot simply spill oil to test scenarios. Until models are

developed to be tailored to local 3D circulation, model results can be used in misleading ways. We advocate for more transparency around methods, biases, and assumptions to support accurate interpretation of model results and informed decision making.

4.2. The future of oil in the Salish Sea

We show that different oil types are more likely to impact certain coastlines than others. This spatial variation in oil type impacts is a natural consequence of the geographic variations in oil transfers at marine terminals (partially shown in Part 1 of this manuscript, Mueller et al. (2025), their Figure 6) as well as the different traffic patterns of vessels with different oil capacities (see Mueller et al., 2025, their Figures 2 and 4). Oil transfers and traffic patterns vary with changes in regulations and terminal expansions. Here, we discuss how regulatory changes will affect the transport of persistent oils across the Salish Sea.

Canada's Westridge Marine Terminal exports 60 Aframax tankers (~7,200,000 m^3) of Canada Conventional Crude and Dilbit each year (Kanjilal, 2019). After the completion of the TransMountain expansion project, this volume will increase to 408 Aframax tankers a year, or ~48,960,000 m^3 per year. To our knowledge, Parkland Refinery (the only Canadian refinery in our study domain) does not import crude by marine transport (pers. comm. Bikramjit Kanjlal, June 18, 2020). We estimate that, of crude oil transported across the Salish Sea in 2018, Washington accounts for 72% and Canada accounts for 28%. Assuming that Washington refining has remained similar to the volumes used in this study, the completion of the TransMountain Expansion project opens the possibility of a change in crude oil transport across the Salish Sea such that Canada export of crude from Westridge Marine Terminal could account for 73% of crude export across the Salish Sea and Washington crude export could become only 27% of total crude transport. The expansion of the Westridge Marine Terminal became operational in the first quarter of 2024, with a projected increase in the capacity for crude oil export through the Salish Sea by about 17 million liters per year (Trans Mountain Corporation, 2023). Prior to completion of this project, tanker traffic from Westridge Marine Terminal was expected to increase 7-fold, from 1 tanker per week to around 7 per week (Kanjilal, 2019). We have not evaluated the actual increase in vessel traffic from this terminal.

Terminal expansions to accommodate increased marine shipping of goods will also change the landscape of risk for persistent oils, such as Bunker-C; however, International Maritime Organization (IMO) regulations are causing a shift toward lower-sulfer HFO fuels and Liquid Natural Gas (LNG). According to Statista, 30% of new large-size vessels that are being ordered are LNG (Statista, 2024). If spilled, LNG will evaporate and/or ignite, reducing the marine oiling impacts of traditional fuels but introducing other air pollution and greenhouse gas impacts.

4.3. Asset planning

Typical mechanical recovery uses booms to contain and concentrate oil for skimmers to collect into storage containers. In the Salish Sea, however, the 4-times daily tide current fluctuations introduce lateral gradients in surface current (shear) that can cause equipment failure, resulting in an inability to recover oil. Estimated recovery times under good weather conditions in this area need to include both response times and the length of periods within the tide cycle during which recovery of oil is not possible. In addition to this predictable impediment to recovery, weather conditions may also prevent safe operations for oil spill recovery, which may prevent response vessels from engaging in a response and recovery operation. Having assets in place to respond to an incident only helps if conditions are favorable for response and recovery at the time of a spill. This study shows what the risk of no response looks like but further research is needed to evaluate regional differences in this risk, both from tide-driven currents and likelihood of prohibitive response conditions. The true risk of impacts from oil spills would include this risk of not being able to respond together with incident risk. One area of increased incident risk is the Eastern Juan de Fuca. Here, vessel traffic lanes cross for vessels servicing Vancouver and the Puget Sound. A higher numbers of incidents in this region motivated the Puget Sound Harbor Safety Committee to develop voluntary traffic procedures to help reduce the number of incidents; however, incidents occur at random times and it is not possible to time incidents so they coincide with good conditions for response and recovery. The authors have yet to see studies evaluating oil spill risk based on when and where weather or other environmental conditions would prohibit response operations and see value in combining this evaluation together with incident risk in the Salish Sea.

4.4. Toward reconciliation

This research took place in both the U.S. and Canada on the territories of many Indigenous communities. We acknowledge that some of these territories are unceded while others are governed with treaty rights. These territories encompass a diversity of cultures, people, lands, and ways of living that were taken during colonization, with harmful impacts that continue to this day. There are some unifying experiences from colonization and there are some key differences. One difference between communities is that some communities have treaties and treaty rights with the British crown or U.S. government while others do not. In other words, these territories hold complexities. For researchers, like ourselves, who would like to engage in the work of reconciliation with Indigenous communities, we recommend developing knowledge of communities and treaty rights together with a willingness to allow tribes their right to choose their relationships and to define their own preferences without inadvertently imposing our own. This recommendation may seem obvious, simple, and easy but the challenge lies in the reality that many of us (the authors of this manuscript included) may not be aware of our assumptions and the ways in which we are imposing our beliefs. In this section, we share the aspects of our growth and learning that we see as being more broadly beneficial for other researchers who share our interest in moving science toward advancing in ways that reconcile past harms together with preventing future harms.

Articles like Wong et al. (2020) and Hird et al. (2023) guided our understanding of how to best reconcile harm to our local Indigenous communities through our practice of communicating science; however, we quickly learned that the recommendations in Wong et al. (2020) were not preferred by our local communities. We had not yet developed the relationships and trust necessary to contribute in the ways that we thought would be preferred. Science and scientists have perpetuated harm to Indigenous communities and this historical context means that we are not automatically seen as trustworthy. We can expect a need to earn trust by developing relationships over time. Beyond developing personal relationships with community members, Institutional Review Boards (IRBs) across North America function as decision-making authorities, through which collaborations are approved or declined. We reached out to some of ours for guidance on local preferences. The North West Indian College IRB recommended that we and other researchers seek to offer communities support by asking tribal researchers questions like:

1. How can I best support your work with mine?
2. What is the best way to present our research to you to help support you and your work?

Asking these questions is a way of acknowledging that colonizers have asked for and taken a lot from these communities and that our role in reconciling this past harm is to fix this imbalance of power by moving toward supporting rather than extracting. The University of British Columbia offers a free course on Indigenous Reconciliation that is a good starting point for developing this awareness of what supportive,

informed, and respectful practices can look like. An important consideration is that any advancement of relationships needs to be on their terms and each community holds different values and priorities.

Prior to reaching out to Indigenous researchers or IRBs, non-Indigenous researchers can work toward respectful relationships by:

1. Taking a course to learn about our history and respectful relations
2. Developing knowledge of communities and their relationship with the land
3. Developing knowledge of the tribal perspective on treaty rights
4. Presenting science in relatable units to communities (e.g. gallons for tribes within U.S. borders)
5. Developing an awareness of culturally important locations and tailoring scientific information to show impacts to these locations
6. Offering information freely

Our efforts to advance reconciliation in this manuscript are reflected in (a) presenting science in relatable units for communities, (b) showing results in a way that highlights the impact on culturally important locations, and (c) insisting that our research is provided in a freely accessible way. Regarding relatable units, we present oil volume in liters for Canadian Indigenous communities and provide a version with units that are used by U.S. tribes (e.g. gallons, available upon request from the authors).

Showing our results in a way that highlights the impact on culturally important locations was difficult because a culturally important beach may be 30 m long but our model grid cell size is ~500 m by ~500 m. In addition, the goal of this study was to present information on the likelihood of impacts. We attempt to reconcile these incongruities by creating maps that compare spill locations that affect selected coastlines to those that do not (see Fig. 9). Rather than naming the territories included in these selections, we refer non-Indigenous to maps of territories (see, e.g., Native Land Digital, 2023). We invite co-development and refinement of this work in collaboration with Tribes and community researchers.

5. Conclusion

We have presented results from a Monte Carlo simulation of 10,000 spills that were statistically generated from AIS data and oil transfer data and that evolved as individual spill scenarios under the influence of Salish Sea hydrodynamics (SalishSeaCast, Soontiens et al., 2016; Soontiens and Allen, 2017; Olson et al., 2020), waves (Wave Watch III®, Gemmrich and Pawlowicz, 2020), winds (HRDPS, Milbrandt et al., 2016; Environment and Climate Change Canada, 2019), and oil weathering (MOHID, Neves, 2013; Marine and Environmental Technology Research Center, 2015; MIDOSS Research Group, 2018; Li, 2017). The method for generating these spills is documented in Mueller et al. (2025) and referred to as the Study Spill Set. A goal of this study was to evaluate the risks from crude oil transport because crude oil contains more environmental toxins, can sink to irrecoverable depths, and can emulsify to ~3x the spill volume. Our results highlight potential risks from 2018 marine oil transport with crude oil modeled as Alaska North Slope crude and other persistent and non-persistent oils represented as Bunker-C and Diesel, respectively.

The region most likely to experience coastal oiling by persistent oils like ANS and Bunker-C as well as oiling of the surface of the water or in the water column is the eastern Juan de Fuca Strait, through Haro Strait, with another "hot spot" just north of Orcas Island. Vertical mixing due to tidal currents through Haro Strait and Boundary Pass results in an average depth of naturally dispersed oil in the water column of around 50 m. Both Diesel and Bunker-C also present a high likelihood of coastal impacts in pockets of the Puget Sound and more narrow waterways, like Fraser River.

Regional impacts vary by oil type. ANS is the least likely oil to impact the coastlines, but also the oil type with the greatest beached oil by volume along the at-risk coastline. The geometric mean volume along the coastline (representing the most likely volume) is most similar to the geometric mean volume maps of Bunker-C and Diesel, which shows that these two oil types are most likely to be spilled and to impact the coastlines.

Time to arrival on coastlines is generally a function of distance to coastline with shorter arrival times in more narrow waterways and longer arrival times in more broad waterways. This oil arrival time is different than response or recovery time because response and recovery time must take into account the reality that booms and skimmers are less effective or ineffective under certain periods of the tide cycle and in situations of strong and opposing currents (shear) or wave action. In certain areas, response times aimed at protecting coastlines may need to be much quicker than the most likely oil arrival times presented here in order to get ahead of tide-induced currents or weather conditions. Average beaching times are commonly less than four days with many coastal areas likely affected by oiling in less than a day.

The previously mentioned relationship between time to coastal oiling and distance to shoreline may lead some to believe that distance to shoreline is a good measure to use for regulating protections; however, we show that distance to shoreline does not necessarily predict the likelihood of impact for any given spill. To the contrary, our maps for spills that impact a selected region vs. those that do not impact the selected region highlight that there are factors other than distance-to-shore that shape spill trajectory, namely, ocean circulation. Creating no-traffic areas will prevent oil spills from occurring within the boundaries but cannot protect sensitive regions from the advection and transport of oil into the boundary through ocean circulation.

Protecting Salish Sea marine resources from oil spill impacts will require further development of modeling tools for evaluating risks and impacts. These include comparison studies of oil spill fate using different hydrodynamic models (e.g. Regional Ocean Modeling System and Finite Volume Community Ocean Model) and the development of oil spill fate parameterizations that reflect local conditions. Comparing output from different modeling platforms will be an important step toward understanding if and how these maps of risk and likelihood are influenced by model configuration and architecture. Updating oil spill fate algorithms to reflect Salish Sea conditions (e.g. strong tide convergence fronts) rather than open ocean conditions will also better tailor model design to this region. Further research is also needed to define the likelihood of spill origin in order to support the protection of sensitive cultural and ecological areas. We recommend implementing a standard for assessing the fate and risk of oil in the Salish Sea that includes the use of hydrodynamic models like SalishSeaCast that capture circulation influences from seasonally variable freshwater discharge and tides, with accessible documentation of model evaluation, inputs, and configuration.

6. Open research section

SalishSeaCast, HRDPS, and WW3 model output used in MOHID model runs is accessible through ERDDAP at https://salishsea.eos.ubc.ca/erddap/index.html. Washington state oil transfer data is publicly accessible by request through https://ecology.wa.gov/Footer/Public1445-records-requests. Aggregated model output from MOHID is accessible through The Federated Research Data Respository at https://doi.org/10.20383/103.01353. All software used to develop this manuscript is available through GitHub (MIDOSS research team, 2024). Python 3.6 - 3.12 was used to pre- and post-process model output. Figures were made with Matplotlib version 3.8.2 (Hunter, 2007), available under the Matplotlib license at https://matplotlib.org/. The Miniconda coding environment can be replicated using https://github.com/MIDOSS/MuellerEtAl_MIDOSS_paper/blob/main/envs/monte_carlo.yaml. Maps were created with Cartopy 0.22.0 (Met Office, 2010). Code for this project is licensed under either Apache 2.0 (https://en.wikipedia.org/wiki/Apache_License.in) or GNU licenses(https://www.gnu.org/licenses/old-licenses/gpl-2.0.en.html#SEC1), as specified on the repositories.

CRediT authorship contribution statement

Rachael D. Mueller: Writing – original draft, Writing – review & editing, Visualization, Supervision, Resources, Investigation, Data curation, Validation, Software, Methodology, Formal analysis, Conceptualization. **Susan E. Allen:** Writing – review & editing, Validation, Software, Project administration, Investigation, Formal analysis, Conceptualization, Visualization, Supervision, Resources, Methodology, Funding acquisition, Data curation. **Stephanie Chang:** Writing – review & editing, Resources, Methodology, Funding acquisition, Supervision, Project administration, Investigation, Conceptualization. **Haibo Niu:** Software, Project administration, Investigation, Formal analysis, Supervision, Resources, Methodology, Funding acquisition, Conceptualization. **Douglas J. Latornell:** Supervision, Project administration, Investigation, Conceptualization, Software, Methodology, Data curation. **Shihan Li:** Writing – review & editing, Software, Investigation, Data curation, Validation, Methodology, Formal analysis, Conceptualization. **Ryah Bagshaw:** Methodology, Formal analysis, Investigation, Data curation. **Ashutosh Bhudia:** Software, Methodology, Formal analysis, Resources, Investigation, Conceptualization. **Vicky Do:** Software, Methodology, Formal analysis, Visualization, Resources, Investigation, Conceptualization. **Krista Forysinski:** Software, Investigation, Conceptualization, Methodology, Data curation. **Ben Moore-Maley:** Visualization, Methodology, Funding acquisition, Software, Investigation, Conceptualization. **Cameron Power:** Visualization, Resources, Investigation, Data curation, Software, Methodology, Formal analysis, Conceptualization.

Funding

This project was funded under Marine Environment Observation Prediction and Response (MEOPAR) (Grant number 37.1 and an unnumbered knowledge mobilization grant) and by Digital Research Alliance of Canada Resource Allocation Competition grants RRG 1541 and 1792.

Declaration of competing interest

The authors declare that they have no known competing financial interests or personal relationships that could have appeared to influence the work reported in this paper.

Acknowledgments

We are incredibly grateful to all those who contributed to this work but would like to especially thank Ramiro Neves and the MOHID development team for providing an open-source model that supports full transparency and allowed for the development of this work. The first author would also like to thank Susan Allan's MOAD research group for their patience and support of my learning Python for the purpose of this work. Of those not listed as co-authors, I particularly benefited from the support of Tereza Jarnikova and Karyn Suchy. A special thanks to Amy MacFadyen for her review and thoughtful comments on this manuscript. Thanks as well to Chris Barker, Dylan Righi, and Dalina Thrift-Viveros for sharing knowledge on oil chemistry, spills, and response. Lastly, the critical eyes and comments of two anonymous reviewers helped refine this paper in important ways, and we are incredibly grateful for their input.

This work took place on the territories of the xʷməθkʷəy̓əm (Musqueam or "place of the məθ kʷəy̓ flower") First Nation and the federally recognized Lhaq'temish (Lummi or "People of the Sea") and Nooksack ("always bracken fern roots") nations. These tribes have stewarded these lands since time immemorial and have rights to the governance of these lands and waterways that the authors of this paper are beginning to learn more about. We developed our understanding of how we can advance science together with reconciliation for indigenous communities during this project and have tailored the presentation of our results to better meet community preferences and needs. A special thanks to the community members who took the time to help guide and support my understanding of how I could best serve community needs with this research.

The information in this paper reflects the views of the author, and does not necessarily reflect the official positions or policies of NOAA or the Department of Commerce.

Appendix A. Supplementary data

Supplementary material related to this article can be found online at https://doi.org/10.1016/j.marpolbul.2025.118410.

Data availability

Access to our research code is available at zenodo repositories (with doi) as cited in the manuscript.

References

Aalberg, A.L., Bye, R.J., Ellevseth, P.R., 2022. Risk factors and navigation accidents: A historical analysis comparing accident-free and accident-prone vessels using indicators from AIS data and vessel databases. Marit. Transp. Res. 3, 100062.

Allen, S.E., 2021. Bootstrap method. https://github.com/MIDOSS/Visualization/blob/main/notebooks/Incremental_Sums.py.

Allen, S.E., Soontiens, N.K., Dunphy, M., Olson, E.M., Latornell, D.J., 2025. Controls on exchange through a tidal mixing hotspot at an estuary constriction. J. Phys. Oceanogr. 55, 415–433.

Canada Energy Regulator, 2023. Pipeline profiles: Trans mountain. https://www.cer-rec.gc.ca/en/data-analysis/facilities-we-regulate/pipeline-profiles/oil-and-liquids/pipeline-profiles-trans-mountain.html#throughput.

Chauvin, C., Lardjane, S., Morel, G., Clostermann, J.-P., Langard, B., 2013. Human and organisational factors in maritime accidents: Analysis of collisions at sea using the HFACS. Accid. Anal. Prev. 59, 26–37.

Council of Canadian Academies, 2016. Commercial Marine Shipping Accidents: Understanding the Risks in Canada. Technical Report, Council of Canadian Academies.

Czuba, J.A., Magirl, C.S., Czuba, C.R., Grossman, E.E., Curran, C.A., Gendaszek, A.S., Dinicola, R.S., 2011. Sediment Load from Major Rivers into Puget Sound and its Adjacent Waters. US Department of the Interior, US Geological Survey.

Dillon Consulting, 2017. Area Risk Assessment Final Report: Southern Portion of British Columbia Pilot Area. Technical Report, Transport Canada.

Downing, E., 2021. Nathan E. Stewart oil spill: Five years after. https://clearseas.org/en/blog/nathan-e-stewart-oil-spill-five-years-after/.

Duran, R., Romeo, L., Whiting, J., Vielma, J., Rose, K., Bunn, A., Bauer, J., 2018. Simulation of the 2003 foss barge-point wells oil spill: A comparison between BLOSOM and GNOME oil spill models. J. Mar. Sci. Eng. 6 (3), 104.

EBA Engineering Consultants, 2013. Modelling the Fate and Behavior of Marine Oil Spills for the TransMountain Expansion Project. Technical Report, Tetra Tech Company.

Environment and Climate Change Canada, 2019. High resolution deterministic prediction system. URL: http://data.ec.gc.ca/data/weather/products/high-resolution-deterministic-prediction-system/. (Accessed 2019).

Environment and Climate Change Canada, 2022. A catalogue of crude oil and oil product properties (1999) - revised 2022. https://data-donnees.az.ec.gc.ca/data/substances/scientificknowledge/a-catalogue-of-crude-oil-and-oil-product-properties-1999-revised-2022/?lang=en.

Fay, J.A., 1969. The spread of oil slicks on a calm sea. In: Oil on the Sea. Springer, pp. 53–63.

Fernandes, R., Braunschweig, F., Lourenço, F., Neves, R., 2016. Combining operational models and data into a dynamic vessel risk assessment tool for coastal regions. Ocean. Sci. 12 (1), 285–317.

Fingas, M.F. (Ed.), 2011. Oil Spill Science and Technology. Elsevier.

Fingas, M.F., 2015. Handbook of Oil Spill Science and Technology. Wiley Online Library.

Flores, H., Saavedra, I., Andreatta, A., Llona, G., 1998. Measurements of oil spill spreading in a wave tank using digital image processing. WIT Trans. Ecol. Environ. 20, 165–173. http://dx.doi.org/10.2495/OIL980151.

Gemmrich, J., Pawlowicz, R., 2020. Wind waves in the Strait of Georgia. Atmos.-Ocean 58 (2), 79–97.

Hare, J., 2021. UBCx: Reconciliation through Indigenous education. https://www.edx.org/learn/education/university-of-british-columbia-reconciliation-through-indigenous-education.

Hauser, D.D., Glenn, R.T., Lindley, E.D., Pikok, K.K., Heeringa, K., Jones, J., Adams, B., Leavitt, J.M., Omnik, G.N., Schaeffer, R., et al., 2023. Nunaaqqit Savaqatigivlugich—working with communities: evolving collaborations around an Alaska Arctic observatory and knowledge hub. Arct. Sci. 9 (3), 635–656.

Hird, C., David-Chavez, D.M., Gion, S.S., van Uitregt, V., 2023. Moving beyond ontological (worldview) supremacy: Indigenous insights and a recovery guide for settler-colonial scientists. J. Exp. Biol. 226 (12).

Hunter, J.D., 2007. Matplotlib: A 2D graphics environment. Comput. Sci. Eng. 9 (3), 90–95. http://dx.doi.org/10.5281/zenodo.10150955.

Johansen, Ø., Reed, M., Bodsberg, N., 2015. Natural dispersion revisited. Mar. Poll. Bull. 93, 20–26. http://dx.doi.org/10.1016/j.marpolbul.2015.02.026.

Jones, P.W., 2018. A user's guide for SCRIP: A spherical coordinate remapping and interpolation package. https://github.com/SCRIP-Project/SCRIP/wiki/SCRIP-User-Guide.

Kanjilal, B., 2019. Trans mountain expansion project. Salish Sea Shared Waters Forum.

Keramea, P., Spanoudaki, K., Zodiatis, G., Gikas, G., Sylaios, G., 2021. Oil spill modeling: A critical review on current trends, perspectives, and challenges. J. Mar. Sci. Eng. 9 (2), 181.

Kimmerer, R.W., Artelle, K.A., 2024. Time to support Indigenous science. Science 383 (6680), http://dx.doi.org/10.1126/science.ado0684, 243–243.

Latornell, D., et al., 2019. Monte Carlo spill characteristic generator. https://github.com/MIDOSS/MOHID-Cmd/blob/main/mohid_cmd/monte_carlo.py.

Li, S., 2017. Evaluation of New Weathering Algorithms for Oil Spill Modeling. (Master's thesis). Dalhousie University, http://hdl.handle.net/10222/73100.

Li, K.X., Yin, J., Fan, L., 2014. Ship safety index. Transp. Res. Part A: Policy Pr. 66, 75–87.

Lyman, W., Reehl, W., Rosenblatt, D., 1982. Handbook of Chemical Property Estimation Methods, vol. 171, McGraw Hill.

Mackay, D., 1980. A mathematical model of oil spill behaviour. Technical Report, Environment Canada, Environmental Protection Service, Environmental Impact, Report EE-7.

Mackey, E., Fletcher, A., Cousins, K., 2022. Nature's Value in the Salish Sea: Non-Market Benefits and Human Well-Being. Technical Report, Earth Economics, Tacoma, WA.

Madec, G., the NEMO team, 2016. NEMO Ocean Engine. Technical Report, Institut Pierre-Simon Laplace (IPSL).

MARETEC, 2019. MOHID modelling system description. http://maretec.mohid.com/PortugueseEstuaries/Reports/MOHID_Description.pdf. (Accessed 07 November 2019).

Marine and Environmental Technology Research Center, 2015. https://github.com/Mohid-Water-Modelling-System.

Met Office, 2010. Cartopy: a cartographic python library with a Matplotlib interface, Exeter, Devon. URL: https://scitools.org.uk/cartopy.

MIDOSS Research Group, 2018. https://github.com/MIDOSS/MIDOSS-MOHID-CODE.

MIDOSS research team, 2024. Source code for: A statistical representation of oil spill fate in the Salish Sea. http://dx.doi.org/10.5281/zenodo.10939120, https://github.com/MIDOSS/MuellerEtAl_MIDOSS_paper/blob/main/README.md.

MIDOSS team, 2022. random_oil_spills.py. https://github.com/UBC-MOAD/moad_tools/blob/main/moad_tools/midoss/random_oil_spills.py.

Milbrandt, J.A., Bélair, S., Faucher, M., Vallée, M., Carrera, M.L., Glazer, A., 2016. The pan-Canadian high resolution (2.5 km) deterministic prediction system. Weather. Forecast. 31 (6), 1791–1816.

Mueller, R.D., Allen, S.E., Chang, S., Niu, H., Latornell, D., Li, S., Bagshaw, R., Bhudia, A., Do, V., Forysinski, K., Moore-Maley, B., Power, C., 2025. A statistical representation of oil spill fate in the Salish Sea (Part 1). Marine Poll. Bull. (In press).

Mueller, R.D., Allen, S., MIDOSS research team, 2018a. Companion code for Marine Pollution Bulletin 2025 manuscripts: A statistical representation of oil spill fate in the Salish Sea, Parts 1 and 2. In: Marine Pollution Bulletin (Vol. 221). Zenodo. https://10.5281/zenodo.10939119.

Mueller, R.D., Allen, S., MIDOSS research team, 2018b. Part2_Figure3_Fate_MedianErr.ipynb in companion code for marine pollution bulletin 2025 manuscripts: a statistical representation of oil spill fate in the salish sea, parts 1 and 2. In: Marine Pollution Bulletin (Vol. 221). Zenodo. https://10.5281/zenodo.10939119.

Najmi, A., 2015. An introduction to the Poisson bootstrap. URL: https://www.unofficialgoogledatascience.com/2015/08/an-introduction-to-poisson-bootstrap26.html.

Native Land Digital, 2023. Native Land Digital. URL: https://native-land.ca.

Neves, R., 2013. The MOHID concept. In: Mateus, M., Neves, R. (Eds.), Ocean Modeling for Coastal Management – Case Studies with MOHID. IST Press, Lisboa Portugal, pp. 1–11, URL: http://www.mohid.com/PublicData/Products/BookPapers/2013_mohidbook_C01.pdf.

Niu, H., Li, S., Li, P., King, T., Lee, K., 2017. Stochastic modeling of the fate and behaviors of an oil spill in the Salish Sea. Int. J. Offshore Polar Eng. 27 (04), 337–345.

Olson, E.M., Allen, S.E., Do, V., Dunphy, M., Ianson, D., 2020. Assessment of nutrient supply by a tidal jet in the Northern Strait of Georgia based on a biogeochemical model. J. Geophys. Res.: Ocean. 25 (8), http://dx.doi.org/10.1029/2019JC015766.

Page, R., Van Deren, M., Soares, J., Kerr, N., 2019. San Juan County Oil Spill Risk Consequences Assessment. Technical Report, Earth Economics, URL: https://www.sjcmrc.org/media/20625/spill-conseq-assmnt-and-ertv-cost-eval-w-factsheet-sjc-final.pdf.

Pawlowicz, R., Hannah, C., Rosenberger, A., 2019. Lagrangian observations of estuarine residence times, dispersion, and trapping in the Salish Sea. Estuar. Coast. Shelf Sci. 225, 106246.

Pawson, C., 2018. Canadian navy ship spills 30,000 litres of fuel in Strait of Georgia. https://www.cbc.ca/news/canada/british-columbia/hmcs-calgary-fuel-spill-1.4551467.

Reich, D., Etkin, D., Rowe, G., Zamorski, S., 2016. Modeling Oil Spill Trajectories in Baffin Bay and Lancaster Sound. Technical Report, Shoal's Edge Consulting, WWF-Canada.

Ship-source oil pollution Fund, 2017. Zidell Marine 277 & Jake Shearer (2017). URL: https://sopf.gc.ca/wp-content/uploads/pdf/2018-2019%20Incident%20and%20Claims%20Portfolio/Zidell%20Marine%20277%20%20Jake%20Shearer%20-%20120-732-R%20-%20EN%20-%202019-05-03.pdf.

Soontiens, N., Allen, S., 2017. Modelling sensitivities to mixing and advection in a sill-basin estuarine system. Ocean. Model. 112, 17–32. http://dx.doi.org/10.1002/2015JC011118.

Soontiens, N., Allen, S., Latornell, D., Le Souef, K., Machuca, I., Paquin, J.-P., Lu, Y., Thompson, K., Korabel, V., 2016. Storm surges in the Strait of Georgia simulated with a regional model. Atmos.-Ocean 54 (1), 1–21. http://dx.doi.org/10.1080/07055900.2015.1108899.

Statista, 2024. URL: https://www.statista.com/statistics/1296511/global-share-of-lng-fueled-new-ship-orders-by-type/.

Trans Mountain Corporation, 2023. Trans mountain corporation provides update on the expansion project. https://www.transmountain.com/news/2023/trans-mountain-corporation-provides-update-on-the-expansion-project.

Transportation Safety Board of Canada, 2016. Marine transportation safety investigation report M16p0378. https://www.tsb.gc.ca/eng/rapports-reports/marine/2016/m16p0378/m16p0378.html.

Van Dorp, J.R., Merrick, J., 2017. VTRA 2015 Final Report Updating the VTRA 2010: A POTENTIAL Oil Loss Comparison of Scenario Analyses by Four Spill Size Categories. Washington State Department of Ecology Report Washington State Department of Ecology Report 17-08-009, George Washington University and Virginia Commonwealth University.

Venosa, A., Holder, E., 2007. Biodegradability of dispersed crude oil at two different temperatures. Marine Poll. Bull. 54 (5), 545–553.

Visser, A.W., 1997. Using random walk models to simulate the vertical distribution of particles in a turbulent water column. Mar. Ecol. Prog. Ser. 158, 275–281.

Washington State Department of Ecology, 2020. 2018 public record P000735-043020. https://ecology.wa.gov/Footer/Public-records-requests.

Washington State Department of Ecology, 2023. Summary of Tug Escort Analysis Results: Report to the Legislature Pursuant to RCW 88.16.260. Technical Report 23-08-009, Washington State Department of Ecology, Page A-58 in tug escort report describes our "sources of uncertainty".

Wong, C., Ballegooyen, K., Ignace, L., Johnson, M.J.G., Swanson, H., 2020. Towards reconciliation: 10 calls to action to natural scientists working in Canada. FACETS 5 (1), 769–783. http://dx.doi.org/10.1139/facets-2020-0005.

Woodward, P., 2019. Cargo ship acquitted of charges relating to 2015 oil spill. https://www.cbc.ca/news/canada/british-columbia/marathassa-acquitted-charges-2015-oil-spill-1.5010021.

Zhong, X., Li, P., Lin, X., Zhao, Z., He, Q.S., Niu, H., Yang, J., 2022. Diluted bitumen: physicochemical properties, weathering processes, emergency response, and recovery. Front. Environ. Sci. 10, 910365.

Zhong, X., Niu, H., Wu, Y., Hannah, C., Li, S., King, T., 2018. A modeling study on the oil spill of M/V Marathassa in Vancouver harbour. J. Mar. Sci. Eng. 6 (3), 106.